Limnol. Oceanogr., 55(2), 2010, 714–724

A model of phytoplankton acclimation to iron–light colimitation

Erik T. Buitenhuis[a,*] and Richard J. Geider[b]

[a] School of Environmental Sciences, University of East Anglia, Norwich, United Kingdom
[b] Department of Biological Sciences, University of Essex, Colchester, United Kingdom

Abstract

We developed and calibrated a dynamic model for cellular carbon, chlorophyll (Chl), and iron under iron–light colimitation. The model allows growth rate and two other state variables (Fe_p : C and Chl : C) to be described as functions of light intensity and the free iron concentration (Fe′). The model requires specification of the values of nine parameters. We obtained values for these parameters using published experimental results for *Thalassiosira pseudonana* using a combination of a random parameter initialization and a golden section search to minimize the cost function. The tuned model explained 95% of the variability in the observations of growth rate, 94% in Chl : C, and 90% in Fe_p : C. Although the model is applicable to both balanced and unbalanced growth conditions, data were only available for balanced growth; thus, the dynamics of state variables during unbalanced growth conditions could not be investigated. A limitation in calibrating the model was in the scarcity of suitable experimental data sets under well-defined environmental forcing. This points to the need for new experimental work on iron-limited cultures, including measurements of photosynthesis–light curves and the dynamic responses to changed Fe′ and light intensity. This phytoplankton growth model provides a physiological treatment of iron–light colimitation for implementation within ocean biogeochemical models. By including both growth rate and elemental stoichiometry (e.g., Fe_p : C) as state variables, the model can be applied to assess both rate and yield limitation.

Iron is the primary limiting nutrient for both phytoplankton growth rate and export production in about 30% of the ocean, where high concentrations of nitrate are present in surface waters throughout the year (de Baar et al. 2005; Boyd et al. 2007). These are the high-nutrient low-chlorophyll (HNLC) regions. At a physiological scale, iron limitation reduces the rates of CO_2 fixation and inorganic N assimilation of phytoplankton by limiting the capacity of the light reactions of photosynthesis to provide the energy (adenosine-5′-triphosphate) and reducing equivalents (nicotinamide adenine dinucleotide phosphate) needed for these processes (Geider and La Roche 1994). This is largely due to a reduction in the cellular quota of iron-containing components of the photosynthetic electron transfer chain, which constitute the most significant fraction of cellular Fe_p in iron-limited cells (Strzepek and Harrison 2004). At the ecological scale, iron limitation reduces the rate of export production, which is evident as residual concentrations of nitrate and phosphate in surface waters at the end of the growing season. In HNLC regions, much effort has gone into evaluating how iron limitation interacts with light, temperature, and/or grazing using experimental manipulations (de Baar et al. 2005; Boyd et al. 2007; Moore et al. 2007) and evaluating how inputs of iron-rich dust and complexation and scavenging of iron interact with the carbon, nitrogen, and phosphorus cycles using biogeochemical models (Parekh et al. 2005; Aumont and Bopp 2006; Moore and Doney 2007).

A nutrient can be limiting in at least two senses. First, the concentration of a nutrient or its flux into a system may limit the phytoplankton yield. This concept is derived from Liebig's law of the minimum and is often referred to as Liebig limitation. Second, the concentration of a nutrient may limit the rate of phytoplankton growth: this is often referred to as Blackman limitation.

Liebig's law can be paraphrased as follows: the yield of a plant population is limited by the nutrient that is least available relative to the plant's requirement for that nutrient. Liebig's law was originally developed for agriculture (Liebig 1840), specifically for the practical purpose of understanding how augmenting nutrient supply by addition of fertilizers affects crop yield. In the open ocean, the equivalent to fertilization is the introduction of "new" nutrients into a region by water transport or mixing and/or atmospheric deposition. Over a long enough time and large enough area of the open ocean, yield is equivalent to export production. Thus, application of Liebig's law to marine biogeochemistry requires information on the inputs and availability of potentially limiting nutrients as well as the elemental stoichiometry of the export production. In HNLC regions, the supply of iron limits export production in the sense of Liebig's law of the minimum.

Blackman's law states that when a biological process is constrained by "a number of separate factors, the rate of the process is limited by the pace of the 'slowest' factor" (Blackman 1905). Originally developed to account for the effects of CO_2 concentration, H_2O availability, light intensity, and temperature on leaf photosynthesis (Blackman 1905), Blackman's law is implicit in some models of phytoplankton growth where the growth rate is treated as the minimum of the dependence of growth on nutrient concentrations and light intensity, modulated by the temperature dependence of the light and nutrient saturated growth rate. With regard to iron limitation of phytoplankton growth in HNLC regions, Blackman's law would postulate that growth is limited by the concentration of the

* Corresponding author: martinburo@email.com

bioavailable form of Fe′ (Sunda and Huntsman 1997) or a constraint imposed by a physical factor such as temperature or light. Fe′ is the free dissolved inorganic iron concentration, i.e., the dissolved iron that is not complexed by organic ligands or inorganic ions.

Whereas geochemists are often interested in assessing limitation in the sense of Liebig's law, biologists more often focus on limitation in the sense of Blackman's law or exceptions to Blackman's law. The important distinction is between a geochemical yield (e.g., Liebig's law limitation) and a biological rate (Blackman-type limitation). Although it is convenient to work within a framework that treats these two types of limitation as different, this distinction may be blurred in nature. This is the case where there may be a kinetic constraint on the availability of a nutrient such as Fe′ or CO_2, which in turn limits the rate at which another nutrient, such as nitrate or phosphate, can be consumed (e.g., Blackman-type limitation) and thus the ultimate yield (e.g., Liebig-type limitation).

Further complicating the attempt to understand and model nutrient limitation of phytoplankton growth rate in marine systems is the metabolic flexibility of phytoplankton (Arrigo 2005). This is evident as marked variability in the elemental stoichiometry (C : N : P : Fe_p) and pigment : biomass ratio (chlorophyll [Chl] : C) that arises from variability in the availability of limiting and nonlimiting nutrients, as well as light and temperature (Sunda and Huntsman 1995; Anning et al. 2001; Price 2005). This metabolic flexibility is also manifested by variability in the efficiency with which limiting nutrients are used to support biomass accumulation. For example, low irradiance greatly decreases the efficiency of iron use (Sunda and Huntsman 1997). As such, light limitation and iron limitation can be viewed as end members of a continuum that includes varying degrees of colimitation. Although Blackman's law does not allow for colimitation at any given instant in time, one of the factors that Blackman identified as relevant to leaf photosynthesis was leaf chlorophyll content (Blackman 1905). In phytoplankton, colimitation by light and an inorganic nutrient (e.g., N or Fe′) is manifested as a change in the Chl : C ratio. Thus, by including chlorophyll as one of the factors affecting leaf photosynthesis, Blackman (1905) left open the possibility of a mechanism for colimitation to operate over timescales that are long enough for the Chl : C to change (e.g., hours to days or longer). Significantly, iron–light colimitation has been observed in the Southern Ocean (Moore et al. 2007), showing the relevance of this physiological acclimation to ocean biogeochemistry. Such colimitations may be common in the plankton, arising from both biochemical and ecological processes (Arrigo 2005).

Modeling framework. Traditionally, nutrient limitation of phytoplankton growth rate has been treated empirically either as a function of the external nutrient concentration (Monod 1950) or of the internal nutrient quota (reviewed by Droop 1983). More sophisticated models consider both the external concentration and intracellular quota, as exemplified in models developed by Flynn et al. (1997). On the other hand, bio-optical models were developed to account for the effect of light on growth (Kiefer and Mitchell 1983). In these bio-optical models, nutrient limitation acts by reducing Chl : C but may also influence the carbon-specific light-saturated photosynthesis rate and the chlorophyll-specific light-limited photosynthesis rate. Geider et al. (1998) combined the bio-optical approach modified from that used by Kiefer and Mitchell (1983) with a simple treatment of inorganic N assimilation, parameterization of the rate of chlorophyll synthesis as a function of "excitation pressure" on the photosynthetic apparatus, and parameterization of light-saturated photosynthesis as a function of the nitrogen-to-carbon ratio. Moore et al. (2002) extended this approach to include limitation by Fe, P, and Si (for diatoms) as well as N and implemented the model in a one-dimensional biogeochemical model to assess the effects of multiple limiting nutrients. An alternative model of multiple nutrient (N, Fe) limitation was described by Flynn and Hipkin (1999).

The Geider et al. (1998) model was developed for nitrogen–light colimitation. Many phytoplankton show limited capacity for luxury uptake of nitrogen, and thus luxury uptake was not part of the model. However, luxury uptake may be a prominent feature of phytoplankton iron physiology (Sunda and Huntsman 1995; Marchetti 2009). This luxury consumption of iron was the initial reason why we set out to devise a mathematical model of iron–light colimitation that is simple enough for it to be implemented in ocean biogeochemical models. Our starting point was the physiological model of Geider et al. (1998), which we reformulated to apply to iron limitation. In this paper we describe this new model and use it in a zero-dimensional implementation, which only simulates a single point in space but includes acclimation through time, to simulate laboratory physiological experiments. We used a parameter optimization technique to fit the parameters in the model to the experimental results of Sunda and Huntsman (1995, 1997).

Methods

Model description—We adapted the Geider et al. (1998) model of nitrogen–light colimitation to iron limitation as follows (Eqs. 1–5). The symbols are explained in Table 1. First, we allowed for luxury uptake of iron by introducing an optimum Fe_p : C ratio (Q_{opt}). This is one of the features that distinguishes our model from that of Moore et al. (2002). Below the optimum, all of the cellular Fe_p is assumed to be located in functional pools, primarily the components of the photosynthetic electron transfer chain. Above Q_{opt}, additional Fe_p is assumed to be accumulated as a storage product.

Second, the carbon-specific light-saturated photosynthesis rate is assumed to increase linearly with Q between the subsistence quota (Q_{min}) and Q_{opt} (Eq. 1); above Q_{opt}, P^C_{max} remains at its maximum value (Fig. 1A).

$$P^C_{max} = \mu_{max} \times \min\left(\frac{Q - Q_{min}}{Q_{opt} - Q_{min}}, 1\right) \quad (1)$$

Third, the rate of organic carbon, C, accumulation (given by Eq. 2) is proportional to the organic carbon concentration (C).

Table 1. Symbols and model parameters.

Function*	Symbol	Description	Units	*T. pseudonana*†	*T. pseudonana*‡
p	α^{Chl}_{max}	maximum initial slope PE curve	g C m² (g Chl mol photons)$^{-1}$		10.7
p	α^{Chl}	initial slope PE curve	g C m² (g Chl mol photons)$^{-1}$	3.7	
p	θ^{C}_{max}	maximum Chl : C ratio	g g^{-1}	0.049	0.072
p	$\rho^{hi}_{max}/\rho^{lo}_{max}$	ratio between iron-limited and iron-saturated maximum uptake rate	—	29	83
p	*k*	dependence of α^{Chl} on θ^{C}	—		26
p	$K_{1/2}$	half-saturation constant	nmol L^{-1}	75	173
p	μ_{max}	maximum growth rate	d^{-1}	1.85	1.55
p	Q_{min}	minimum Fe_p : C ratio	μmol mol^{-1}	11	12
p	Q_{opt}	optimum Fe_p : C ratio	μmol mol^{-1}	38	31
p	Q_{max}	maximum Fe_p : C ratio	μmol mol^{-1}	293	281
i	*E*	light intensity	μmol photons m^{-2} s^{-1}	50, 500	50, 500
i/*m*§	Fe′	dissolved iron	pmol L^{-1}	15–7547	15–7547
m/*i*§	μ	growth rate=$(1/C)(\delta C/\delta t)$	d^{-1}		
m	θ^{C}	Chl : C ratio	g g^{-1}		
m	C	cellular carbon	mol L^{-1}		
m	Fe_p	cellular iron	μmol L^{-1}		
m	*Q*	Fe_p : C ratio	μmol mol^{-1}		

* *p*, parameter; *i*, independent variable; *m*, model predicted.
† With constant α^{Chl}.
‡ Using Eq. 7.
§ We used a "turbidostat" program, with *E* and Fe′ as independent variables. We also tried a "chemostat" program, with *E* and μ as independent variables, but this did not converge toward an optimized parameter set.

$$\frac{\delta C}{\delta t} = P^{C}_{max} \times \left(1 - \exp\left(\frac{-\alpha^{Chl}\theta^{C}E}{P^{C}_{max}}\right)\right) \times C \qquad (2)$$

In this equation, the biomass specific photosynthesis rate, P^{C}, is assumed to be a function of light (*E*), the chlorophyll-to-carbon ratio (θ^{C}), and P^{C}_{max} through a photosynthesis–light relationship similar to that employed by Geider et al. (1998). Like Geider et al. (1998), we initially assumed that α^{Chl} is a constant that does not depend on any of the state or environmental variables. However, during model calibration, we found that this assumption needed to be revised (*see* Eq. 7 below).

Fourth, we adopted the following relationship (Eq. 3) between Fe′ uptake and the Fe_p : C ratio, which is equation 8 in table 1 of Morel (1987).

$$\frac{\delta Fe_p}{\delta t} = \rho_{max} \times \frac{Fe'}{K_{1/2} + Fe'} \times C \qquad (3)$$

where

$$\rho_{max} = \rho^{hi}_{max} - (\rho^{hi}_{max} - \rho^{lo}_{max}) \times \frac{(Q - Q_{min})}{(Q_{max} - Q_{min})} \qquad (4)$$

Eq. 4 is the same as equation 13 in table 1 of Morel (1987), but with a corrected typographical error (F. Morel pers. comm.). It describes how the maximum rate of iron uptake is down-regulated in response to the accumulation of cellular Fe_p. Such down-regulation of maximum uptake capacity appears to be a common feature of the alleviation of nutrient limitation (Morel 1987). It requires specification of the values of four parameters in addition to μ_{max}. In this

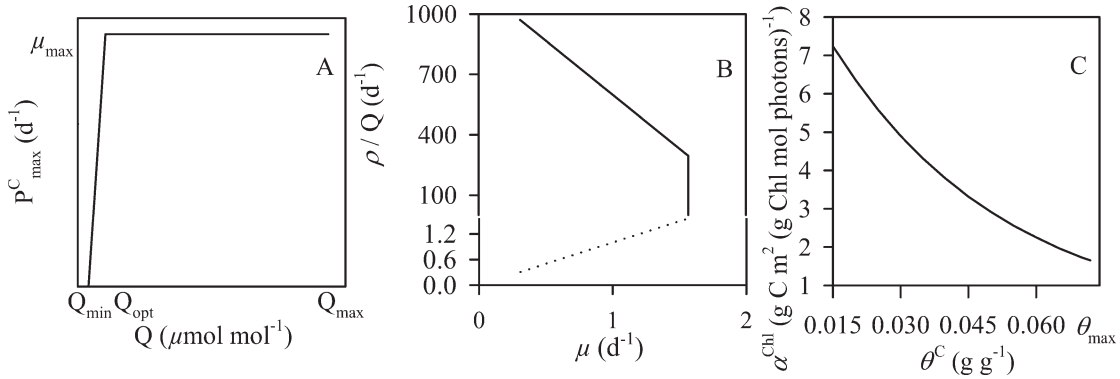

Fig. 1. (A) P^{C}_{max} as a function of Fe_p : C, (B) iron uptake rate as a function of μ. Solid line, ρ_{max}/Q; dashed line, steady-state specific iron uptake rate $(1/Fe_p)(\delta Fe_p/\delta t)$, and (C) α^{Chl} as a function of θ^{C}.

equation, the maximum iron uptake rate is enhanced at low cellular iron content ($Q_{\min}$), while in steady state the actual iron uptake rate is limited by Fe′. The maximum iron uptake rate decreases to the actual iron uptake rate at the maximum Fe_p : C ratio ($Q_{\max}$), which in steady state at $Fe' \gg K_{1/2}$ leads to maximum growth (i.e., $\rho^{\text{lo}}_{\max} = \mu_{\max} Q_{\max}$, which can be obtained by combining equations 10–12 in table 1 of Morel 1987). Both maximum and steady-state iron uptake rates are linear functions of Q (figure 4, top panel in Morel 1987). However, because of our introduction of a Q_{opt} above which growth is at its maximum, $\rho_{\max}$ is no longer a linear function of μ (Fig. 1B, compared to figure 5, bottom panel in Morel 1987).

Finally, chlorophyll synthesis (Eq. 5) is treated in a similar manner to that employed by Geider et al. (1998). However, we use a maximum Chl : C ratio as in Geider et al. (1997), in contrast to the maximum Chl : N ratio in Geider et al. (1998).

$$\frac{\delta \text{Chl}}{\delta t} = \left(P^{\text{C}}_{\max} \times \left(1 - \exp\left(\frac{-\alpha^{\text{Chl}} \theta^{\text{C}} E}{P^{\text{C}}_{\max}} \right) \right) \right)^2 \times \frac{\theta^{\text{C}}_{\max}}{\alpha^{\text{Chl}} \theta^{\text{C}} E} \times C \quad (5)$$

We note that N : C is largely unaffected by iron limitation (Takeda 1998; Price 2005), and thus there is no material effect of using Chl : C instead of Chl : N in this model.

In the absence of data on gross photosynthesis and respiration, we ignore the (carbon) cost of biosynthesis (ζ in Geider et al. 1998). Given the small Fe : C ratio in phytoplankton (10^{-6} to 10^{-3}), the error this introduces is likely to be small. We have no observations of iron–light limitation as a function of temperature, and we have no observations of transients between steady states; therefore we do not include a temperature function or respiration rate, though these could be included as in Geider et al. (1998).

Experimental data—We used the data reported by Sunda and Huntsman (1995, 1997) to calibrate the model. These investigators grew *Thalassiosira pseudonana*, *Thalassiosira oceanica*, and *Emiliania huxleyi* in trace-metal buffered cultures at a range of Fe′ concentrations. Cell abundance was maintained at low enough concentrations so as not to significantly perturb the iron complexation chemistry within the ethylenediaminetetraacetic acid buffered seawater. Illumination was provided on a 14 : 10 light : dark cycle at photon flux densities of 500 and 50 μmol photons m^{-2} s^{-1} for *T. pseudonana* and at intensities of 500 and 175 μmol photons m^{-2} s^{-1} for *T. oceanica* and *E. huxleyi*. Temperature was held constant at 20°C. Growth rate was obtained from the exponential increase in total cell volume in the cultures, as measured by Coulter Counter. Cultures were fully acclimated to the experimental conditions prior to sampling for chlorophyll, particulate C, and particulate Fe_p. Cellular Fe_p and C contents were measured using radioisotopes. As far as we are aware, these are the only data sets that provide information on balanced growth rate, Fe_p : C, and Chl : C for iron-limited cultures grown at more than one irradiance. This is the minimum information needed to calibrate the model. The data set of Price (2005) for *Thalassiosira weissflogii*, although also of high quality, was not used because experiments were conducted at only one photon flux density.

Parameter optimization—We used a combination of a random parameter generation with the golden section approach to minimize the cost function between observations and the model (Kiefer 1953, *see* also http://en.wikipedia.org/wiki/Golden_section_search). When one of the outer points of the golden section had a lower cost function than the inner point, we widened the section. Thus, the only prior limit on the parameter values is that they must be greater than 0.

We applied this approach to the observations for cultures of *T. pseudonana* (Sunda and Huntsman 1997; B. Sunda pers. comm.), *T. oceanica*, and *E. huxleyi* (Sunda and Huntsman 1995). We optimized the eight or nine parameters in the photosynthesis model (Table 1) by optimizing each parameter consecutively with the golden section search, using the optimum from each iteration as the middle range value in the next iteration and iterating until the parameters changed by less than 1‰. The golden section approach has the advantage of being very fast, but it tended to get stuck in local minima. We therefore initialized each search with 100 sets of parameters that were randomly chosen within a range of ± 50% of the optimum parameters from the previous run, and we did 30 runs.

We used light intensity and dissolved iron concentration as the independent variables. We calculated the cost function by comparing the model output to the observations of growth rate, Chl : C, and Fe_p : C. In order to include observations with different magnitudes in the cost function, we normalized the model results to the observations:

$$\text{CF} = \sum \left(\log\left(\frac{\text{model}}{\text{observation}} \right) \right)^2 \quad (6)$$

We plotted the confidence bounds as $(F(\alpha, 2, n_{\text{obs}} - n_{\text{param}}) \times 2/(n_{\text{obs}} - n_{\text{param}}) + 1) \times \text{CF}/\text{CF}_{\text{opt}}$, in which α is the confidence bound, either 0.90 or 0.99; the number of observations n_{obs} is 57 for *T. pseudonana*, 34 for *T. oceanica*, and 60 for *E. huxleyi*; the number of parameters n_{param} is 8; and CF_{opt} is the cost function of the optimum parameter set.

Results

The optimized model for *T. pseudonana* gives reasonable parameter values (Table 1), with values for α^{Chl} and $\theta^{\text{C}}_{\max}$ that are within the range reported for diatoms (Fig. 2), and the model explains 94% of the variability in the observations of growth rate, 93% in Fe_p : C, and 83% in Chl : C (small symbols in Fig. 3). The model becomes unstable when $Q_{\min} \geq Q_{\text{opt}}$ (black areas in Fig. 2), which is obvious from Eq. 1.

Following Sunda and Huntsman (1997) we also tested the parameter optimization omitting experimental data for the cultures in which calculated Fe′ was higher than the solubility of Fe′ (0.75 nmol L^{-1}). This resulted in fairly similar α^{Chl} (3.6 g C m^2(g Chl mol photons)$^{-1}$), $\theta^{\text{C}}_{\max}$

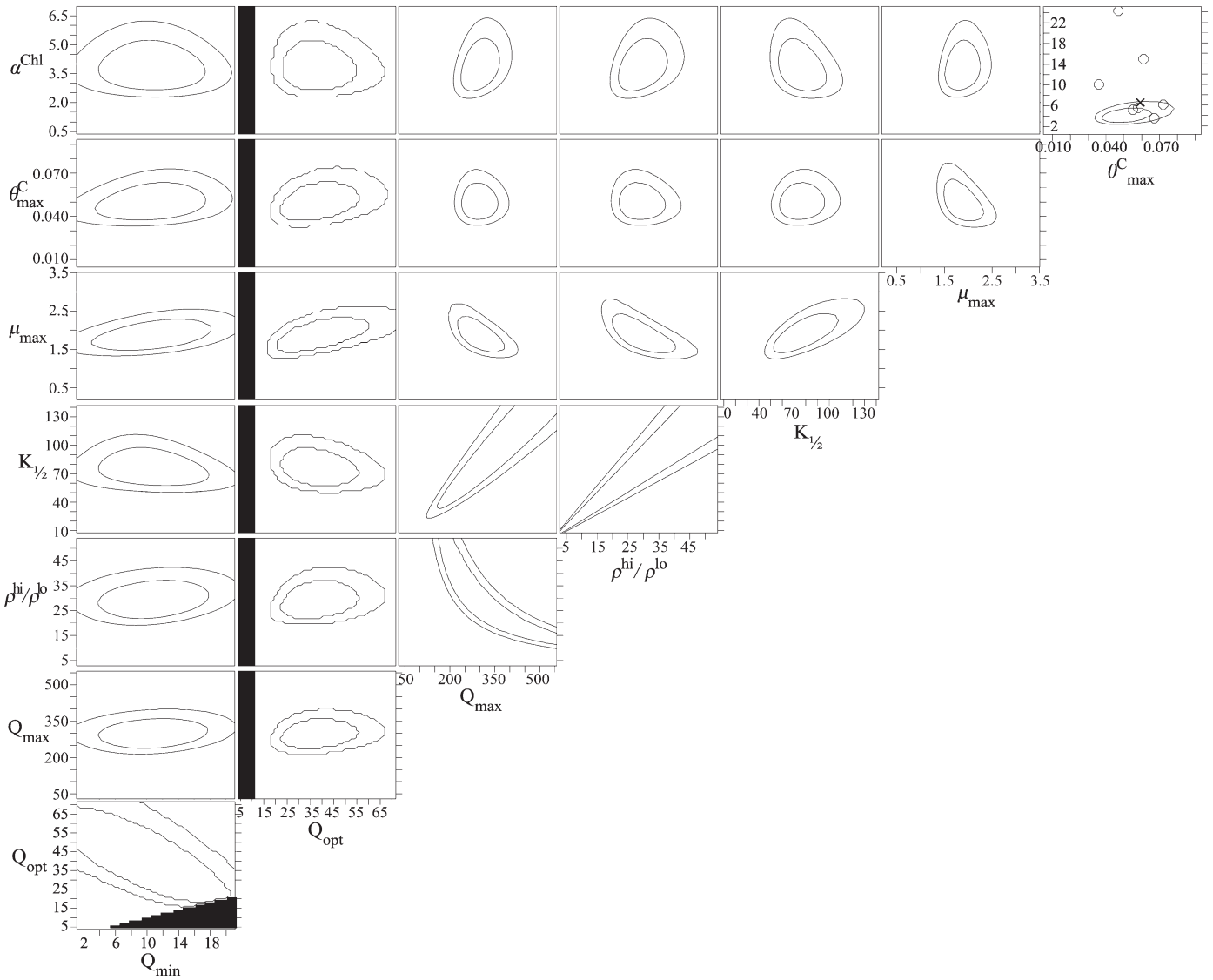

Fig. 2. Confidence bounds of model parameters fit to observations of iron–light colimited cultures of *T. pseudonana*. Contour intervals are 90% and 99%. Q_{min} [μmol mol^{-1}], Q_{opt} [μmol mol^{-1}], Q_{max} [μmol mol^{-1}], ρ^{hi}/ρ^{lo} [-], $K_{1/2}$ [nmol L^{-1}], μ_{max} [d^{-1}], θ^{C}_{max} [g Chl g C^{-1}], α^{Chl} [g C g Chl^{-1} mol photons^{-1}]. Axis ranges are ± 90% from the optimum value, except the plot of θ^{C}_{max} vs. α^{Chl}, in which the range of α^{Chl} has been extended to show the observed parameter range. The model becomes unstable in the black region. The cross indicates θ^{C}_{max} and α^{Chl} as derived from light-limited, iron sufficient cultures of *T. pseudonana*, circles indicate other diatoms (compiled by Geider et al. 1997).

(0.048 g g^{-1}), Q_{min} (13 μmol mol^{-1}), and Q_{opt} (33 μmol mol^{-1}); lower $K_{1/2}$ (37 nmol L^{-1}), μ_{max} (1.69 d^{-1}), and Q_{max} (131 μmol mol^{-1}); and higher $\rho^{hi}_{max}/\rho^{lo}_{max}$ (39).

The main shortcoming of the model as formulated in Eq. 1–5 is that it could not at the same time represent both the big difference in growth rate and the big difference in Chl : C ratio between the high and low light conditions at Fe′ > 500 pmol L^{-1} (Fig. 3). This shortcoming could be largely overcome by making α^{Chl} a function of θ^{C} as follows (Fig. 1C):

$$\alpha^{Chl} = \alpha^{Chl}_{max} \times e^{\left(-k \times \theta^{C}\right)} \quad (7)$$

Although this required the specification of an additional parameter, the marked improvement in match of model with data (Fig. 3, solid lines) appears to warrant this increased complexity, at least for *T. pseudonana*. Eq. 7 was suggested by the relationship between the chlorophyll-specific fluorescence, growth rate, and Chl : C reported for iron-limited *T. weissflogii* by Price (2005). It is consistent with expectations based on a "package effect" on light absorption (Morel and Bricaud 1981).

We also ran the parameter optimization using the Moore et al. (2002) model, which is basically the same as the Geider et al. (1998) model, but with a slightly different formulation of the decrease in the maximum nutrient

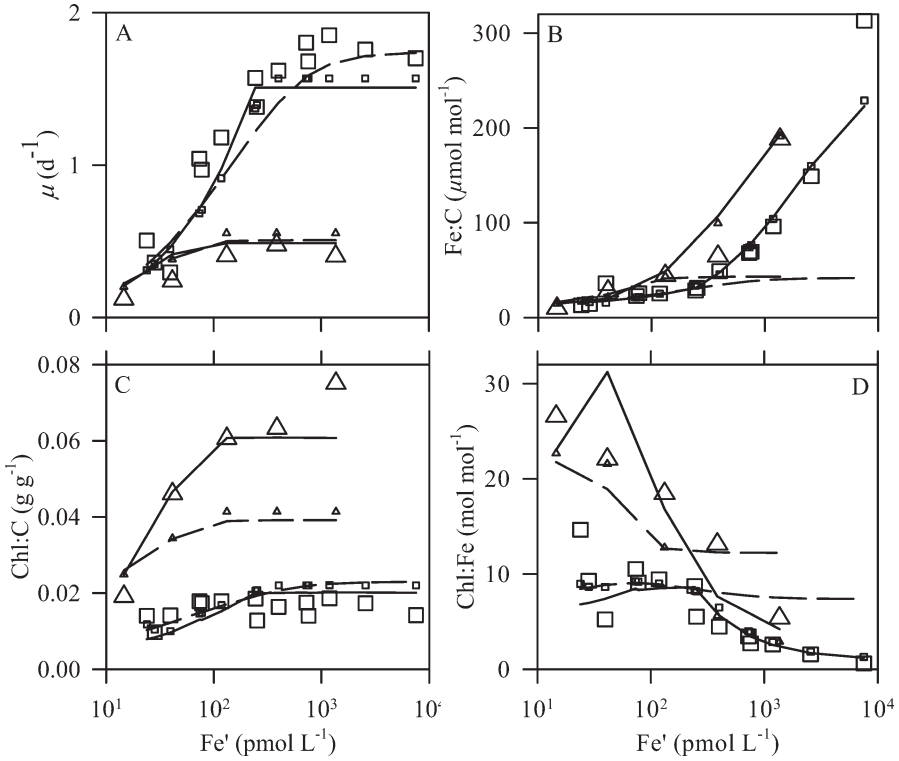

Fig. 3. Observed cell physiology of *T. pseudonana* and model after parameter optimization. Squares, 500 μmol photons m^{-2} s^{-1}. Triangles, 50 μmol photons m^{-2} s^{-1}. Large symbols, observations from Sunda and Huntsman (1997). Small symbols, initial model results. Solid lines, model results with $\alpha^{Chl} = 10.7 \times e^{(-26 \times \theta^C)}$. Dashed lines, results of the Moore et al. (2002) model. Fe′ solubility is 750 pmol L^{-1} (Sunda and Huntsman 1997); thus higher concentrations are "virtual" concentrations in the absence of precipitation.

uptake rate near the maximum nutrient quota (compare equation 7 in table 2 in Geider et al. 1998 with, e.g., equation 84 in Moore et al. 2002). This gave the following parameter values: α^{Chl} (3.3 g C m^2(g Chl mol photons)$^{-1}$), θ^C_{max} (0.044 g g^{-1}), $K_{1/2}$ (4.5 nmol L^{-1}), μ_{max} (4.9 d^{-1}), Q_{min} (0.23 μmol mol^{-1}), and Q_{max} (176 μmol mol^{-1}). The tradeoff between achieving a realistic Fe_p : C ratio and growth rate led to an unrealistic estimate of the maximum growth rate. We therefore excluded the Fe_p : C observations above the Q_{opt} of our eight parameter model (leaving n_{obs} = 48), which gave the following parameter values: α^{Chl} (3.4 g C m^2(g Chl mol photons)$^{-1}$), θ^C_{max} (0.044 g g^{-1}), $K_{1/2}$ (0.39 nmol L^{-1}), μ_{max} (2.3 d^{-1}), Q_{min} (12 μmol mol^{-1}), and Q_{max} (43 μmol mol^{-1}). This gave a much more reasonable fit to the growth rates, Chl : C ratios, and the iron-limited Fe_p : C ratios (Fig. 3, dashed lines).

Table 2. Partially optimized model parameters.

Symbol	*T. oceanica*	*E. huxleyi*
α^{Chl}	11.7*	5.8*
θ^C_{max}	0.079*	0.080*
$\rho^{hi}_{max}/\rho^{lo}_{max}$	29†	29†
$K_{1/2}$	5.2*	1.3*
μ_{max}	1.68‡	1.26‡
Q_{min}	2.5‡	3.7‡
Q_{opt}	3.2*	5.9*
Q_{max}	47‡	45‡

* Obtained by parameter optimization.
† Taken from *T. pseudonana*, Table 1.
‡ Directly taken from experimental results (Sunda and Huntsman 1995).

The parameter optimization did not give physiologically meaningful model parameters for *T. oceanica* and *E. huxleyi*, presumably because the lower light intensity of 175 μmol photons m^{-2} s^{-1} was only low enough to result in an increased Chl : C ratio, but not low enough to give a significant reduction in growth rate (Sunda and Huntsman 1995). In contrast, *T. pseudonana* was grown at a lower, growth-limiting light intensity of 50 μmol photons m^{-2} s^{-1}. We further constrained the optimization of *T. oceanica* and *E. huxleyi* by taking μ_{max}, Q_{min}, and Q_{max} directly from the highest and lowest observed values in the experiments (Sunda and Huntsman 1995). This still led to unrealistic values for $\rho^{hi}_{max}/\rho^{lo}_{max}$ and $K_{1/2}$, with very low values for *T. oceanica* and very high values for *E. huxleyi* (*see* also the strong correlation and poor constraint of this pair of parameters in Fig. 2). Therefore, we used the value of $\rho^{hi}_{max}/\rho^{lo}_{max}$ that was obtained for *T. pseudonana*. We then optimized the remaining parameter values of α^{Chl}, θ^C, $K_{1/2}$, and Q_{opt} (Table 2). The Chl : C ratio for *T. oceanica* and *E. huxleyi* could be described without significant bias (Fig. 4) using the standard model (Eqs. 1–5) without including Eq. 7 (i.e., with constant α^{Chl}). However, these cultures do not constitute an ideal

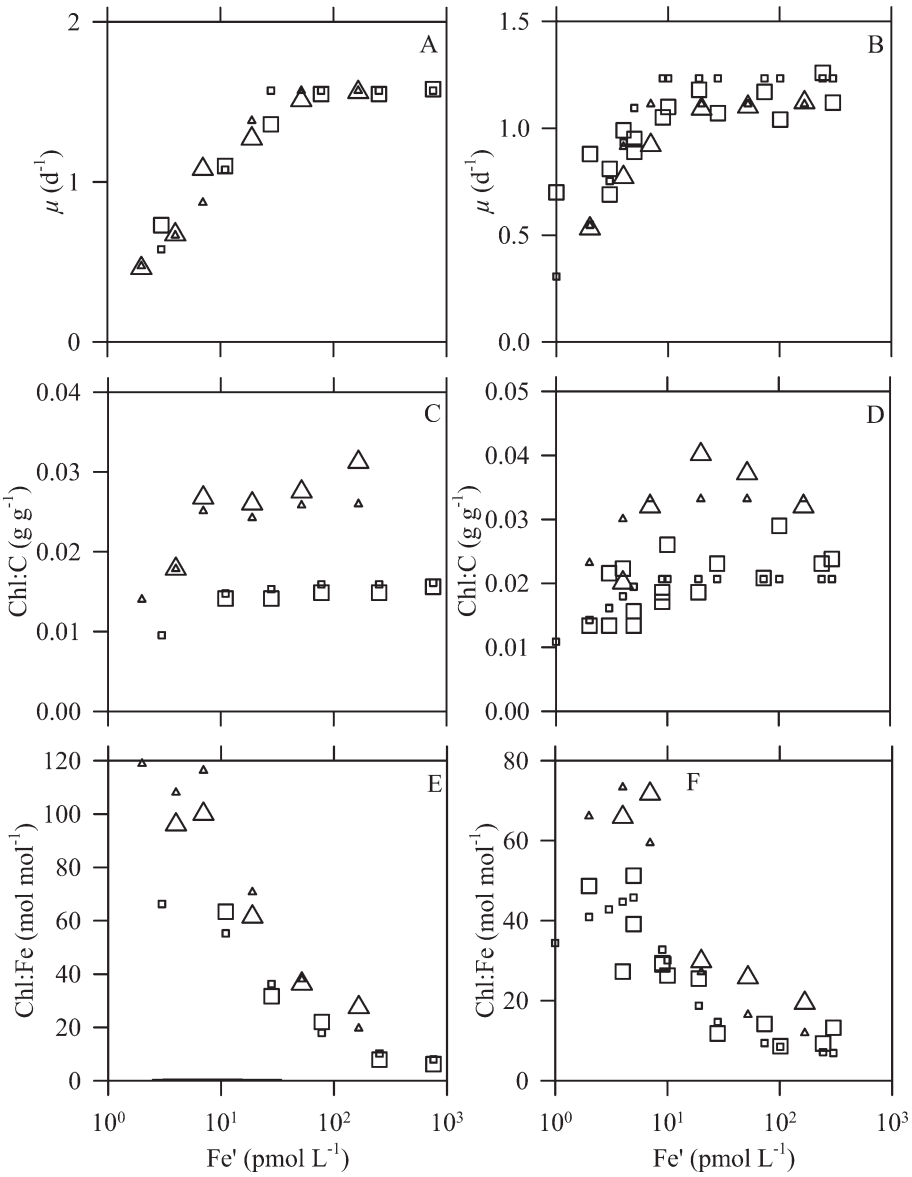

Fig. 4. Observed and modeled cell physiology. Large symbols, observations from Sunda and Huntsman (1995). Small symbol, model results using parameters from Table 2. Squares, 500 μmol photons m^{-2} s^{-1}. Triangles, 175 μmol photons m^{-2} s^{-1}. (A, C, E) *T. oceanica*. (B, D, F) *E. huxleyi*.

test, since the range of light intensities (175 and 500 μmol photons m^{-2} s^{-1}) may not have been sufficient to elicit large enough changes of θ^C to produce a significant enough packaging effect on α^{Chl}. Nonetheless, we cannot rule out the possibility of interspecific variability in relationship of α^{Chl} to θ^C under iron limitation. It would be much more desirable to have direct measurements of α^{Chl} and P^C_{max} from photosynthesis–irradiance (PE) curves than to rely on estimating these parameters from observations of growth rate and Chl : C. Clearly, additional measurements of PE curves will be needed to test whether α^{Chl} varies in iron–light colimited cultures. In the meantime, our model can be used to represent the main features of the physiological adaptations in iron–light colimited cultures.

Discussion

One of the major constraints in developing models of phytoplankton growth and acclimation is the availability of data to both calibrate and validate the models. This is especially the case for iron limitation. We used the high-quality data set of growth rate, carbon, chlorophyll, and iron content for iron-limited and iron-replete *T. pseudonana* at both high and low light of Sunda and Huntsman (1997) to implement a dynamic photosynthesis model of iron–light colimitation. This was the only data set that we are aware of that provides the minimum data set needed to calibrate the model. Validation with an independent data set has not been possible.

Despite the high quality of the Sunda and Huntsman (1997) experimental data, we still lack key information

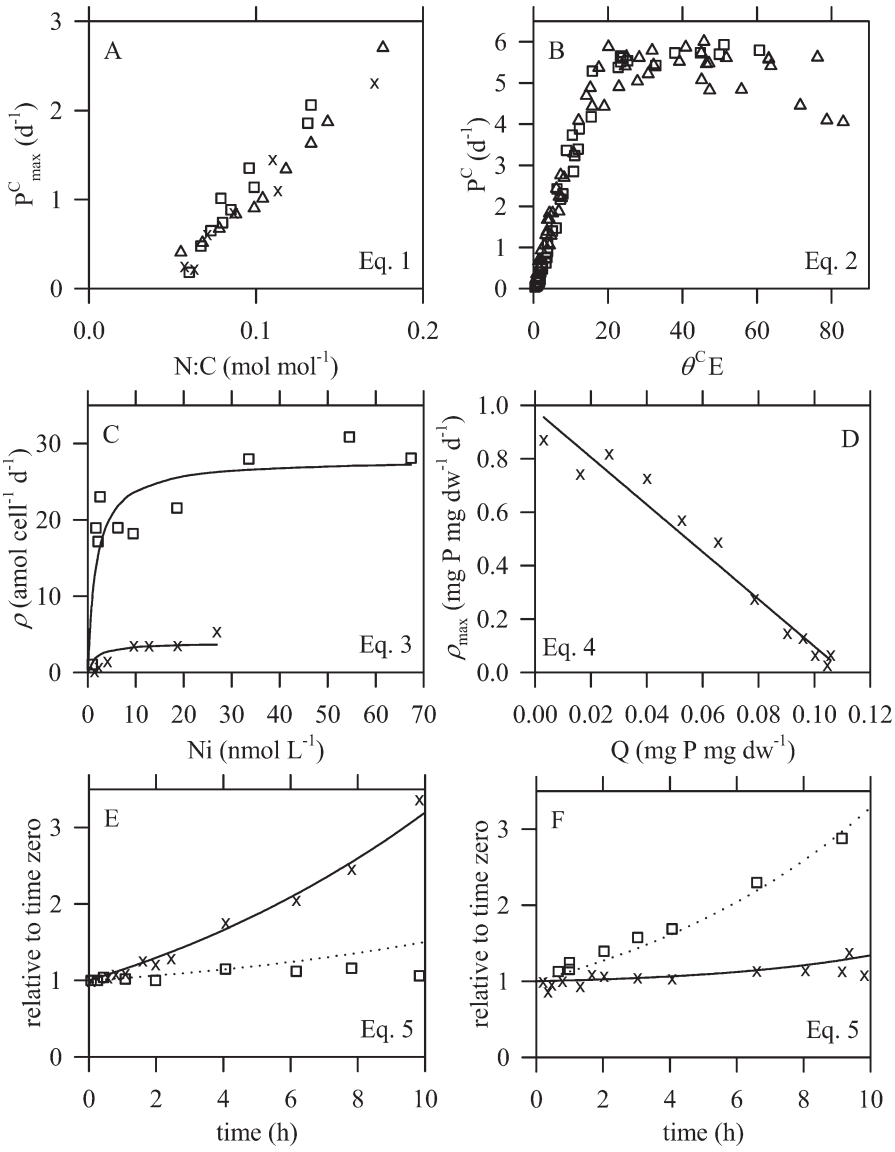

Fig. 5. (A) P^C_{max} as a function of N : C quota; crosses, *P. tricornutum* (Osborne and Geider 1986); triangles, *Isochrysis galbana* (Dubinsky et al. 1986; Herzig and Falkowski 1988); squares, *Pavlova lutheri* (Chalup and Laws 1990). (B) P^C (normalized to "structural carbon", *see* Discussion) as a function of $\theta^C E$ in *Skeletonema costatum* (Anning et al. 2000); squares, high light acclimated; triangles, low light acclimated. (C) Ni uptake rates as a function of Ni concentration in *Synechococcus* sp. strain WH8102 (Dupont et al. 2008); squares, 0.5 nmol L^{-1} Ni acclimated; crosses, 50 nmol L^{-1} Ni acclimated, fit with the following parameters, $K_{1/2}$ (1.8 nmol Ni L^{-1}), $\rho^{0.5}_{max}$ (28 amol Ni $cell^{-1}$ d^{-1}), ρ^{50}_{max} (3.9 amol Ni $cell^{-1}$ d^{-1}). (D) Maximum P uptake rates as a function of P quota in *Prochlorothrix hollandica* (Ducobu et al. 1998). The line is a linear regression through the data, giving the following parameters, $\rho^{hi}_{max}/\rho^{lo}_{max}$ (16), Q_{max} (0.11 mg P mg dry wt^{-1}). (E–F) Light shift experiments. Squares, dotted lines, carbon relative to time zero. Crosses, solid lines, chlorophyll relative to time zero. Squares, crosses, observations of *T. pseudonana* (Cullen and Lewis 1988). Lines, iron-saturated model with the following parameter values, α^{Chl} (6.5 g C m^2 (g Chl mol photons)$^{-1}$), θ^C_{max} (0.074 g g^{-1}), μ_{max} (2.85 d^{-1}). (E) Shift down from 2200 to 100 μmol photons m^{-2} s^{-1}. (F) Shift up from 100 to 2200 μmol photons m^{-2} s^{-1}.

needed to validate the assumptions of the model. In particular, we lack information concerning the effects of iron limitation on the parameters of the photosynthesis–light response curve and on ρ_{max}. As such, our assumption in Eq. 1 that P^C_{max} scales with the Fe_p : C ratio remains untested, as does our assumption that the chlorophyll-specific initial slope, α^{Chl}, can be parameterized as a function of θ^C (Eq. 7) under iron limitation. Further information will also be needed to resolve whether the variation of the chlorophyll quota with iron–light colimi-

Table 3. Observations of growth, photosynthesis, and reaction center contents of Fe-replete and Fe-limited *P. tricornutum* based on data presented in Greene et al. (1991). P^{Fe}_{max} was calculated based on the Fe contained in RCI (12 Fe : RCI) and RCII (2 Fe : RCII).

	Units	Fe replete	Relative SD (%)	Fe limited	Relative SD (%)
Growth rate	d^{-1}	1.5	No data	0.2	No data
RCII : cell	amol cell^{-1}	0.95	15	0.12	10
RCI : cell	amol cell^{-1}	0.33	23	0.03	17
C : cell	pg C cell^{-1}	13	10	9.3	11
P^{cell}_{max}	pmol O_2 (cell s)$^{-1}$	17	15	1.7	13
P^{RCI}_{max}	μmol O_2 (mol RCI s)$^{-1}$	0.51	27	0.58	26
P^{Fe}_{max}	mmol O_2 (mol Fe in RCI + RCII s)$^{-1}$	29		29	
α^{Chl}	mol O_2 m^2 (mol Chl mol photons)$^{-1}$	400	16	530	11

tation needs to be reformulated. These assumptions can be tested with new experimental work.

In addition, the model is inherently dynamic and can be applied to unbalanced growth following perturbations in light intensity and/or Fe′ supply. The main differences between the present model and the Geider et al. (1998) model are, first, that the present model allows for luxury uptake of iron at high dissolved iron concentrations. This is an obvious feature of the Sunda and Huntsman (1997) data set. The second difference is that the Morel (1987) formulation we used here leads to a several times faster increase in Fe_p : C during an upshift in iron concentration, thanks to the enhanced maximum uptake rate at a low Fe_p : C ratio. However, data are only available for steady-state balanced growth conditions, and so this faster dynamic response has not been validated. Testing the dynamics is particularly important because the storage and mobilization of intracellular inorganic iron pools (e.g., ferritin) are likely to be important to the success of phytoplankton in regions of the ocean where the supply of iron is episodic (Marchetti et al. 2009).

The Moore et al. (2002) model implicitly assumes that luxury uptake of Fe does not occur. By including this in our model, it better reproduces the large observed changes in Fe : C ratios (Fig. 3B). This also allows our model to better reproduce the changes in Fe : Chl ratios (Fig. 3D). Like our model without Eq. 7, the Moore et al. (2002) model fails to give realistic Chl : C in low light (Fig. 3C).

Given that all the observations for *T. pseudonana* were necessary to formulate and parameterize the model, and the incomplete validation of the model results with the observations for the other two species, we first briefly reiterate the literature that shows the validity of each of our equations in the eight parameter model for elements other than iron, and then reiterate measurements that suggest Eq. 1 may be valid for iron as well. The linear relationship between P^{C}_{max} and Q (Eq. 1) was clearly shown (Fig. 5) by Geider et al. (1998). The decreasing light requirement proportional to increasing Chl : C (Eq. 2) was shown by Anning et al. (2000) on a cellular basis. In the next paragraph we note that their results are consistent with using this formulation on a carbon basis over a full light : dark cycle. The nutrient uptake rate as a saturating function of external nutrient concentration (Eq. 3) was shown by Dupont et al. (2008). The nutrient uptake rate as a linear function and Q (Eq. 4) was shown by Ducobu et al. (1998). Geider et al. (1996) showed the general validity of the chlorophyll synthesis equation (their figure 4) using the data of Cullen and Lewis (1988). In Fig. 5 we show that these data can also be successfully fit to our iron-saturated model (Eqs. 2 and 5).

We reinterpret the data of Anning et al. (2000) to suggest that Eq. 2 accurately describes photosynthesis. Anning et al. (2000) show that P^{cell} as a function of Chl/cell $\times$ E is the same at low and high light (their figure 5D) and that the difference in P^{C} ($=1/C\ \delta C/\delta t$) is due to a transient increase in cell carbon during the light period, which is then followed by nitrogen uptake and cell division during the dark period, in other words, that the extra carbon is an energy reserve. Here we note that P^{C} (measured in the middle of the light period) normalized to the structural carbon content of the cell (measured at the end of the dark period) is the same at low and high light (Fig. 5B). Effectively, this simplifies the photosynthesis model by attributing the dark nitrogen uptake and cell division to the light period, making it unnecessary to model an energy reserve pool over a 24-h period.

As far as we are aware, there are no available data sets examining the relationship between the photosynthesis–light curve parameters and Fe : C for any microalgae. However, Greene et al. (1991) provide data that support our assumption that the light-saturated photosynthesis rate depends on cellular Fe associated with the photosynthetic electron transfer chain under Fe-limited conditions. Specifically, Greene et al. (1991) measured photosynthesis rates, reaction center I (RCI) : cell and RCII : cell for Fe-replete and Fe-limited *Phaeodactylum tricornutum*. They observed that the cell-specific P^{cell}_{max}, RCI : cell and RCII : cell declined by approximately tenfold under Fe-limited conditions (Table 3). If, as we assumed for the model, the main Fe-pool under Fe limitation is the photosynthetic electron transfer chain and luxury uptake of Fe is in the form of an Fe-storage compound rather than in Fe-containing catalysts, then the observations of Greene et al. (1991) can be interpreted to support the model formulation. We also note that Greene et al. (1991) observed that α^{Chl} increased slightly (by about 33%) under Fe limitation. Thus, Fe limitation in *P. tricornutum* resulted in a large reduction of P^{cell}_{max}, which was proportional to the changes in the Fe-containing RCI and RCII, with a small change in α^{Chl}.

We have used a zero-dimensional model to show that a model with three state variables and eight parameters can

explain 83–94% of the variability that has been measured in the Chl : C ratio, Fe_p : C ratio, and growth rate in cultures of *T. pseudonana*. By adding a ninth parameter, describing the dependence of α^{Chl} to Chl : C, we increased the variability of Chl : C that could be accounted from 83% to 94%. Despite the fact that the parameters were poorly constrained for *T. oceanica*, by optimizing four parameters, the model could explain 95–98% of the variability in the observations. On the other hand, for *E. huxleyi*, the model could explain only 65–74% of the variability in the observations, as a result of the larger scatter in the observations for this species.

In subsequent work, E. Buitenhuis and C. Le Quéré (unpubl. data) will implement this dynamic photosynthesis model in a global ocean biogeochemical model. In ocean biogeochemical modeling, one of the open questions that require the reconciliation of rate limitation (Blackman 1905) and yield limitation (Liebig 1840) is the challenge of reproducing both high plankton productivities and high standing stocks, given the relatively well constrained ecological transfer efficiencies (E. Buitenhuis, R. Rivkin, S. Sailley, and C. Le Quéré unpubl. data). Here, we have attempted to construct a phytoplankton growth model that can be used to ground resolution of this biogeochemical question in information that is available from physiological research.

Our analysis clearly illustrates that new experimental data on both steady-state cultures in balanced growth and cultures subjected to transients in Fe supply are needed to improve our understanding of how to describe Fe–light colimitation of phytoplankton growth. We believe that the best strategy for collecting new experimental data is with a view to testing the assumptions and performance of mechanistic models, such as the one that we propose in this paper.

Acknowledgments

We thank Bill Sunda for providing the observational data, in particular the unpublished Fe′ for low light cultures of *T. pseudonana*. We also thank Graham Upton (University of Essex) and Katrina Morrow (University of Essex) for helpful discussions of parameter estimation using the golden section approach. We thank the reviewers for their detailed comments. This research was supported by the U.K. Natural Environment Research Council through the Marine Quantification of Earth System Feedbacks (MARQUEST) project (NE/C516087/1 to R.J.G. and NE/C516079/1 to E.T.B.) and the European Union through the CarboOcean project (511176[GOCE] to E.T.B.). For programs of parameter optimization and making plots see the additional information at http://lgmacweb.env.uea.ac.uk/green_ocean/.light0D.html.

References

Anning, T., G. Harris, and R. J. Geider. 2001. Thermal acclimation in the marine diatom *Chaetoceros calcitrans* (Bacillariophyceae). Eur. J. Phycol. **36:** 233–341.

———, H. L. Macintyre, S. M. Pratt, P. J. Sammes, S. Gibb, and R. J. Geider. 2000. Photoacclimation in the marine diatom *Skeletonema costatum*. Limnol. Oceanogr. **45:** 1807–1817.

Arrigo, K. R. 2005. Marine microorganisms and global nutrient cycles. Nature **437:** 349–355.

Aumont, O., and L. Bopp. 2006. Globalizing results from ocean in situ iron fertilization studies. Glob. Biogeochem. Cycles **20:** GB2017, doi:10.1029/2005GB002591.

Blackman, F. F. 1905. Optima and limiting factors. Ann. Bot. **19:** 281–295.

Boyd, P. W., and others. 2007. Mesoscale iron enrichment experiments 1993–2005: Synthesis and future directions. Science **315:** 612–617.

Chalup, M. S., and E. A. Laws. 1990. A test of the assumptions and predictions of recent microalgal growth models with the marine phytoplankter *Pavlova lutheri*. Limnol. Oceanogr. **35:** 583–596.

Cullen, J. J., and M. R. Lewis. 1988. The kinetics of algal photoadaptation in the context of vertical mixing. J. Plankton Res. **10:** 1039–1063.

de Baar, H. J. W., and others. 2005. Synthesis of iron fertilization experiments: From the iron age in the age of enlightenment. J. Geophys. Res. Oceans **110:** 1–24.

Droop, M. R. 1983. 25 years of algal growth kinetics. Bot. Mar. **26:** 99–112.

Dubinsky, Z., P. J. Falkowski, and K. Wyman. 1986. Light harvesting and utilization by phytoplankton. Plant Cell Physiol. **27:** 403–434.

Ducobu, H., J. Huisman, R. R. Jonker, and L. R. Mur. 1998. Competition between a prochlorophyte and a cyanobacterium under various phosphorus regimes: Comparison with the Droop model. J. Phycol. **34:** 467–476.

Dupont, C. L., K. Barbeau, and B. Palenik. 2008. Ni uptake and limitation in marine *Synechococcus* strains. Appl. Environ. Microb. **74:** 23–31.

Flynn, K., M. Fasham, and C. Hipkin. 1997. Modelling the interactions between ammonium and nitrate uptake in marine phytoplankton. Philos. Trans. R. Soc. Lond. B **352:** 1625–1645.

———, and C. R. Hipkin. 1999. Interactions between iron, light, ammonium and nitrate: Insights from the construction of a dynamic model of algal physiology. J. Phycol. **35:** 1171–1190.

Geider, R. J., and J. La Roche. 1994. Mini-review: The role of iron in phytoplankton photosynthesis, and the potential for iron-limitation of primary productivity in the sea. Plant Cell Environ. **39:** 275–301.

———, H. L. Macintyre, and T. M. Kana. 1996. A dynamic model of photoadaptation in phytoplankton. Limnol. Oceanogr. **41:** 1–15.

———, ———, and ———. 1997. Dynamic model of phytoplankton growth and acclimation: Responses of the balanced growth rate and the chlorophyll a: Carbon ratio to light, nutrient-limitation and temperature. Mar. Ecol. Prog. Ser. **148:** 187–200.

———, ———, and ———. 1998. A dynamic regulatory model of phytoplanktonic acclimation to light, nutrients, and temperature. Limnol. Oceanogr. **43:** 679–694.

Greene, R. M., R. J. Geider, and P. G. Falkowski. 1991. Effect of iron limitation on photosynthesis in a marine diatom. Limnol. Oceanogr. **36:** 1772–1782.

Herzig, R., and P. G. Falkowski. 1988. Nitrogen limitation in *Isochrysis galbana* (Haptophyceae). I. Photosynthetic energy conversion and growth efficiencies. J. Phycol. **25:** 462–471.

Kiefer, D. A., and B. G. Mitchell. 1983. A simple, steady-state description of phytoplankton growth based on absorption cross-section and quantum efficiency. Limnol. Oceanogr. **28:** 770–776.

Kiefer, J. 1953. Sequential minimax search for a maximum. P. Am. Math. Soc **4:** 502–506, doi:10.2307/2032161.

Liebig, J. von. 1840. Organic chemistry in its applications to agriculture and physiology. Taylor and Walton.

Marchetti, A., and others. 2009. Ferritin is used for iron storage by bloom-forming marine pennate diatoms. Nature **457:** 467–470.

Monod, J. 1950. The technique of continuous cultures: Theory and applications. Ann. Inst. Pasteur, Lille **79:** 390–410, [In French.]

Moore, C. M., S. Seeyave, A. E. Hickman, J. T. Allen, M. I. Lucas, H. Planquette, R. R. Pollard, and A. J. Poulton. 2007. Iron-light interactions during the CROZet natural iron bloom and EXport experiment (CROZEX) I: Phytoplankton growth and photophysiology. Deep-Sea Res. II **54:** 2045–2065.

Moore, J. K., and S. C. Doney. 2007. Iron availability limits the ocean nitrogen inventory stabilizing feedbacks between marine denitrification and nitrogen fixation. Glob. Biogeochem. Cycles **21:** GB2001, doi:10.1029/2006GB002762.

———, ———, J. A. Kleypas, D. M. Glover, and I. Y. Fung. 2002. An intermediate complexity marine ecosystem model for the global domain. Deep-Sea Res. II **49:** 403–462.

Morel, A., and A. Bricaud. 1981. Theoretical results concerning light absorption in a discrete medium, and application to specific absorption of phytoplankton. Deep-Sea Res. **28:** 1375–1393.

Morel, F. M. M. 1987. Kinetics of nutrient uptake and growth in phytoplankton. J. Phycol. **23:** 137–150.

Osborne, B. A., and R. J. Geider. 1986. Effects of nitrate-nitrogen limitation on photosynthesis in the diatom *Phaeodactylum tricornutum* (Bacillariophyceae). Plant Cell Environ. **9:** 617–625.

Parekh, P., M. J. Follows, and E. A. Boyle. 2005. Decoupling of iron and phosphate in the global ocean. Glob. Biogeochem. Cycles **19:** GB2020, doi:10.1029/2004GB002280.

Price, N. M. 2005. The elemental stoichiometry and composition of an iron-limited diatom. Limnol. Oceanogr. **50:** 1159–1171.

Strzepek, R. F., and P. J. Harrison. 2004. Photosynthetic architecture differs in coastal and oceanic diatoms. Nature **431:** 689–692.

Sunda, W. G., and S. A. Huntsman. 1995. Iron uptake and growth limitation in oceanic and coastal phytoplankton. Mar. Chem. **50:** 189–206.

———, and ———. 1997. Interrelated influence of iron, light and cell size on marine phytoplankton growth. Nature **390:** 389–392.

Takeda, S. 1998. Influence of iron availability on nutrient consumption ratios of diatoms in oceanic waters. Nature **393:** 774–777.

Associate editor: Anthony Larkum

Received: 21 April 2009
Accepted: 19 October 2009
Amended: 04 December 2009